

Air-Stable PbSe Nanocrystals Passivated by Phosphonic Acids

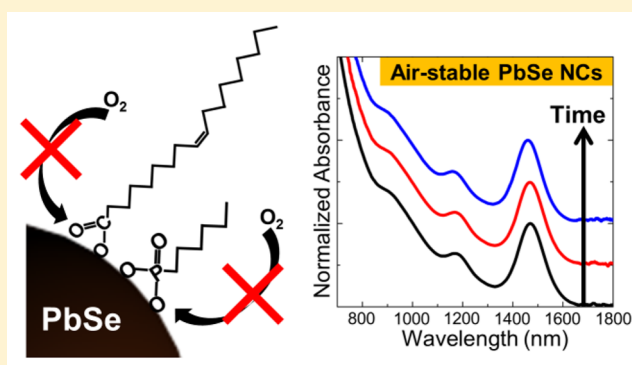
Ju Young Woo,^{†,‡} Soho Lee,[‡] Seokwon Lee,[‡] Whi Dong Kim,[‡] Kangha Lee,[‡] Kyungnam Kim,[†] Hye Jin An,[†] Doh C. Lee,^{*,‡} and Sohee Jeong^{*,†}

[†]Nanomechanical Systems Research Division, Korea Institute of Machinery and Materials (KIMM), Daejeon 305-343, Korea

[‡]Department of Chemical and Biomolecular Engineering (BK21+ Program), KAIST Institute for the Nanocentury, Korea Advanced Institute of Science and Technology (KAIST), Daejeon 305-338, Korea

Supporting Information

ABSTRACT: We developed a new chemical strategy to enhance the stability of lead selenide nanocrystals (PbSe NCs) against oxidation through the surface passivation by P–O– moieties. In the synthesis of PbSe NCs, tris(diethyl-amino)phosphine (TDP) selenide (Se) was used as a Se precursor, and the resulting PbSe NCs withstood long-term air exposure while showing nearly no sign of oxidation. Nuclear magnetic resonance (NMR) spectroscopy reveals that TDP derivatives passivate the surface of PbSe NC. Through a series of ligand cleavage reactions, we found that the TDP derivatives are bound on NC surface through the P–O– moiety. Based on such understanding, it turned out that direct addition of various PAs during the synthesis of PbSe NCs also results in the NCs whose absorption spectrum remains nearly intact after air exposure for weeks. The P–O– moieties render the NCs stable in the operation of field effect transistors, suggesting that our findings can enable the use of air stable PbSe NCs in wider array of optoelectronic applications.



INTRODUCTION

Considerable progress has been made during the past decade in the study of optoelectronic devices based on lead chalcogenide nanocrystals (NCs). One of the most studied materials is PbSe NCs, which exhibit strong quantum confinement effect over a wide range of size because of the relatively large exciton Bohr radius (46 nm) of PbSe.^{1,2} High carrier multiplication (CM) efficiency in PbSe NCs has stimulated the use of the NCs in various optoelectronic devices ranging from photodiodes to photovoltaic cells.^{3–9} However, chemical instability of PbSe NCs against oxidation upon air exposure has impeded the development of optoelectronic devices based on PbSe NCs.^{10–12} For example, PbSe NCs synthesized using trioctylphosphine selenide (TOPSe) degrade rapidly and uncontrollably even after brief air exposure.^{13,14} For this reason, it is required to prepare stable PbSe NCs for successful integration of the NCs into reliable devices.

Strategies to alleviating the instability have derived from observation that surface atoms of PbSe NCs undergo oxidation to yield oxides, e.g., PbO, PbSeO₃, and SeO₂, even in dark.¹² One way to passivate the surface of PbSe NCs is to coat the NCs with inorganic shell. Pietryga et al. reported the growth of CdSe shell on PbSe NCs via cation exchange.¹⁵ While the inorganic shell leads to PbSe core significantly more stable against oxidation, the use of PbSe/CdSe core/shell NCs in devices is limited largely due to the fact that the CdSe shell tends to serve as a barrier for charge transfer between NCs. On

the other hand, Bae et al. reported the surface passivation of PbSe NCs by using molecular chlorine (Cl₂).¹¹ Surface Se atoms of PbSe NCs are replaced with Cl atoms upon the Cl₂ treatment and the Cl₂-treated PbSe NCs showed significantly improved ambient stability. However, the high reactivity of Cl₂ results in etching of PbSe surface, rendering it difficult to control the size of resulting PbSe NCs.

Recently, the use of halide-containing chemicals has facilitated the progress in the preparation of air-stable PbSe NCs. For example, Beard and co-workers reported *in situ* synthesis of air-stable PbSe NCs using Pb halide precursors, PbX₂ (X = Br, Cl, and I).¹⁶ Highly improved air stability of PbSe NCs synthesized from PbX₂ was demonstrated by UV–vis absorption and photoluminescence (PL) spectroscopy. Halide passivated PbSe NCs were also prepared via cation exchange from metal selenide NCs, e.g., CdSe and ZnSe, as seed materials.^{17,18} The PbSe NCs prepared using halide-containing chemicals and precursors show stability against oxidation even when the NCs are in film or in device form.

We recently capitalized on the premise by developing an approach to halide passivation of PbSe NCs.¹⁰ Halide salts injected to PbSe NC growth solution turn the resulting PbSe NCs ultrastable against oxidation even under operation in a field-effect transistor (FET). However, the halide-treated PbSe

Received: October 1, 2015

Published: December 29, 2015

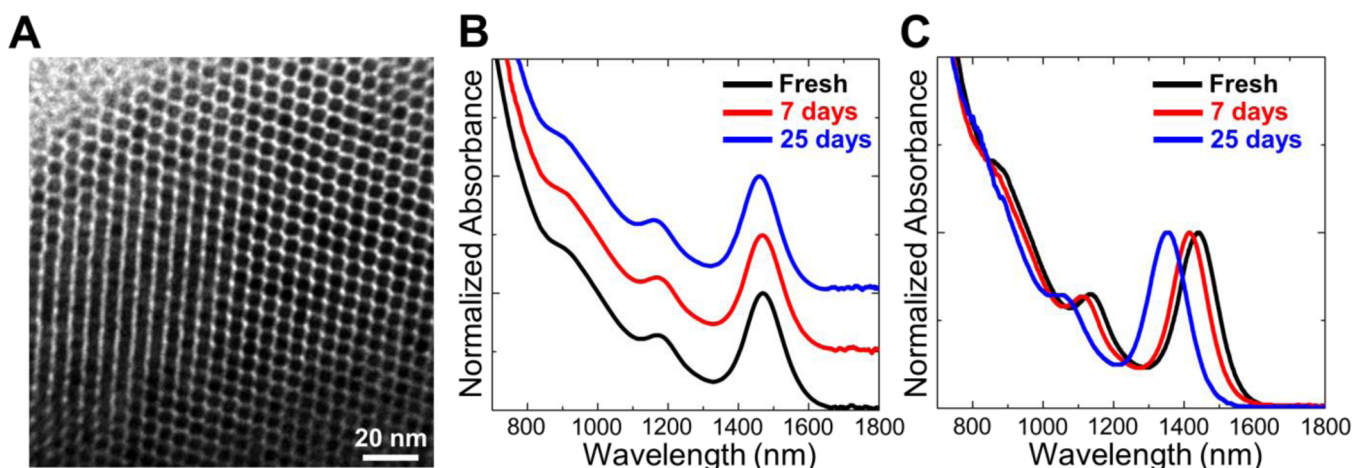


Figure 1. (A) TEM image of PbSe NCs synthesized using TDP (TDP-PbSe NCs). Absorption spectra of (B) TDP-PbSe NCs and (C) TOP-PbSe NCs dispersed in tetrachloroethylene. Absorption spectra were taken at different times between 0 and 25 days after synthesis under air exposure in ambient condition.

NCs showed n-type characteristics,^{10,19–21} ultimately limiting their versatility in the use of p–n junctions. In this sense, it is desired to develop an approach to synthesizing air-stable PbSe NCs without relying on the use of halide as a stabilizing agent.

In this study, we present a new strategy to improve the air stability of PbSe NCs. Tris(diethylamino)phosphine (TDP) was introduced as a selenium source in the form of TDPSe instead of trioctylphosphine selenide (TOPSe), the most widely used Se precursor. The change of Se precursor results in drastically enhanced air stability of PbSe NCs. We carried out ³¹P{¹H} NMR and FTIR spectroscopy to identify surface molecules on PbSe NCs synthesized using TDPSe. The characterizations reveal that P–O– moieties are formed on the PbSe NCs. Various phosphonic acids (PAs) were tested as capping ligands in order to probe the effect of phosphorus-containing molecules on the stability of the surface against oxidation.

RESULTS AND DISCUSSION

Figure 1A shows a TEM image of PbSe NCs synthesized using TDPSe as a Se source (denoted hereafter as TDP-PbSe NCs) after modifying a recipe that involves TOPSe.²² TDPSe was injected to Pb oleate solution, and then highly monodisperse PbSe NCs were obtained (see [Experimental Section](#) for details). From the TEM analysis, the TDP-PbSe NCs appear to form long-range superlattices. This large-scale assembly of the NCs was formed simply by drop-casting NCs hexane solution onto a TEM grid and letting hexane evaporate under ambient conditions, an indication of very narrow size distribution of TDP-PbSe NCs (see [Figure S1](#)). Faster decomposition of TDPSe than that of TOPSe is likely responsible for the narrower size distribution in TDPSe-based synthesis.²³

More importantly, TDP-PbSe NCs did not undergo noticeable shift in absorption spectrum and degradation of PL quantum yield (PL QY) after air exposure as shown in [Figure 1B](#) and [Figure S2](#), respectively. The 1S exciton peak position of TDP-PbSe NCs remains unaltered after air exposure for longer than 25 days, while PbSe NCs synthesized using TOPSe (TOP-PbSe NCs) undergo severe oxidation as clearly confirmed by drastic blue-shift in the absorption spectrum ([Figure 1C](#)). TDP-PbSe NCs show air stability nearly

comparable to halide-treated PbSe NCs (see [Figure S3](#) for the comparison). To the best of our knowledge, this is the first synthesis of air-stable PbSe NCs without introducing halide. It is noted that we also observed notably enhanced air stability in PbSe nanorods (NRs) synthesized using TDPSe ([Figure S4](#)).

Previously, TDPSe was used in the synthesis of PbSe nanorods (NRs).^{24,25} It was revealed that bis(diethylamido)-phosphorous acid (BDPA) is formed during the reaction by hydrolysis of TDP with residual water or oleic acid (OA). BDPA plays a pivotal role in altering the aspect ratio of PbSe NRs.²⁵ However, the effect of TDP or its derivatives on NC surfaces and stability of TDP-PbSe NCs or NRs have been nearly unexplored.

Assuming that TDP interacts with surface of PbSe NCs, one can surmise that the following may have to do with the enhanced stability: (i) rearrangement of surface atoms upon introduction of TDP or (ii) effective passivation of surface dangling bonds by TDP or its derivatives. To examine the possibility of (i), we carried out crystallographic analysis of TDP- and TOP-PbSe NCs. It has been documented that oleate-passivated (111) facets of PbSe NCs are more resistive toward oxidation than (100) planes, hence the size dependency in air stability of PbSe NCs.¹⁰ In certain size regimes, PbSe NCs become more stable as their size gets smaller, because in that size range Wulff construction likely leads to a larger population of more stable (111) facets with decreasing NC size.²⁶ The interaction of TDP with surface atoms of PbSe might result in the varying facet populations in the resulting TDP-PbSe NCs. To examine the hypothesis, we compared integrated peak intensity in X-ray diffraction (XRD) patterns of TOP- and TDP-PbSe NCs.²⁷ As shown in [Figure 2A](#), both TOP- and TDP-PbSe NCs exhibit an identical rock salt PbSe structure with nearly the same integrated peak ratio ((111)/(200) is 0.43 and 0.41 for TOP- and TDP-PbSe NCs, respectively). [Figures 2B](#) and [2C](#) show representative HRTEM images of TOP-PbSe and TDP-PbSe NCs, respectively. The same PbSe(200) lattice spacing and similar quasi-spherical shape were observed for both TOP- and TDP-PbSe NCs. Because the facet ratio has much to do with PbSe NC morphology, the shape similarity is indicative of the same surface structure.^{26,27} Therefore, XRD and TEM analyses strongly suggest that TOP- and TDP-PbSe NCs have nearly identical structure, leading us to exclude the

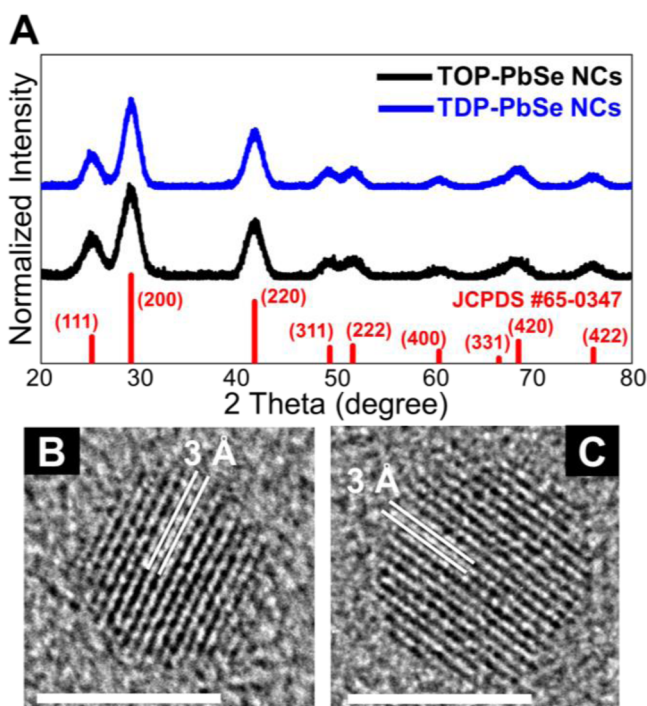


Figure 2. (A) XRD patterns of TOP- and TDP-PbSe NCs. Both patterns are well matched with bulk rock salt PbSe pattern taken from JCPDS #65-0347 (red lines). High-resolution TEM images of (B) TOP-PbSe NCs and (C) TDP-PbSe NCs. Both NCs exhibit lattice spacing of 3 Å, which is in line with lattice spacing of PbSe (200). Scale bars are 5 nm.

possibility of structure-induced enhanced stability in TDP-PbSe NCs.

Figures 3A and 3B show $^{31}\text{P}\{^1\text{H}\}$ NMR spectra of TDP- and TOP-PbSe NCs. Broad resonances in the spectrum of TDP-PbSe NCs (Figure 3A), as well as PbSe NRs (Figure S4), indicate the existence of surface bound phosphorus species, which is contrasted by no peak in the case of TOP-PbSe NCs (Figure 3B).^{28,29} In addition, ligand coverage estimation based on ^1H NMR spectra reveals that oleate is still a predominant ligand, whose surface areal density is comparable to that of TOP-PbSe NCs (Figure S5). We then added bis(trimethylsilyl)sulfide ((TMS)₂S) into benzene-*d*₆ solution of TDP-PbSe NCs to peel the ligands off from NC surface following the ligand cleavage study reported in a previous study on phosphonic acid (PA) capped CdSe NCs.²⁸ Upon mixing, the TDP-PbSe NC solution formed aggregation. $^{31}\text{P}\{^1\text{H}\}$ NMR spectroscopic analysis after this step reveals that the resonance peaks are now significantly sharpened and are upfield shifted compared to the original singlet peak of bound species (Figure 3C).

The ligand cleavage experiments using (TMS)₂S and ensuing NMR analysis indicate that the surface bound species are not TDP but likely its derivatives. This premise is based on the energetic estimation (bond dissociation energy for Si–S and Si–P are 619.0 and 363.6 kJ/mol, respectively); therefore, (TMS)₂S would not be able to cleave TDP from the NC surface.^{30,31} Mixing TDP or TDPSe with (TMS)₂S did not yield noticeable reaction, another corroborating evidence that the bound species on the TDP-PbSe NC surface is not TDP (Figure S6).

Previous studies describing ligand cleavage study of PA-capped CdSe NCs using (TMS)₂S or (TMS)₂Se reveal that

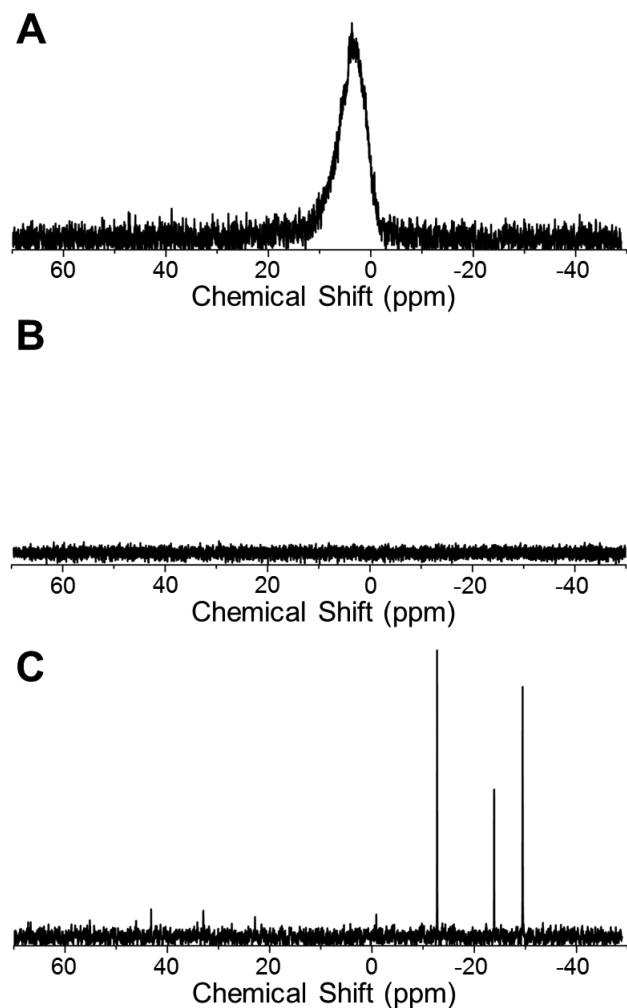
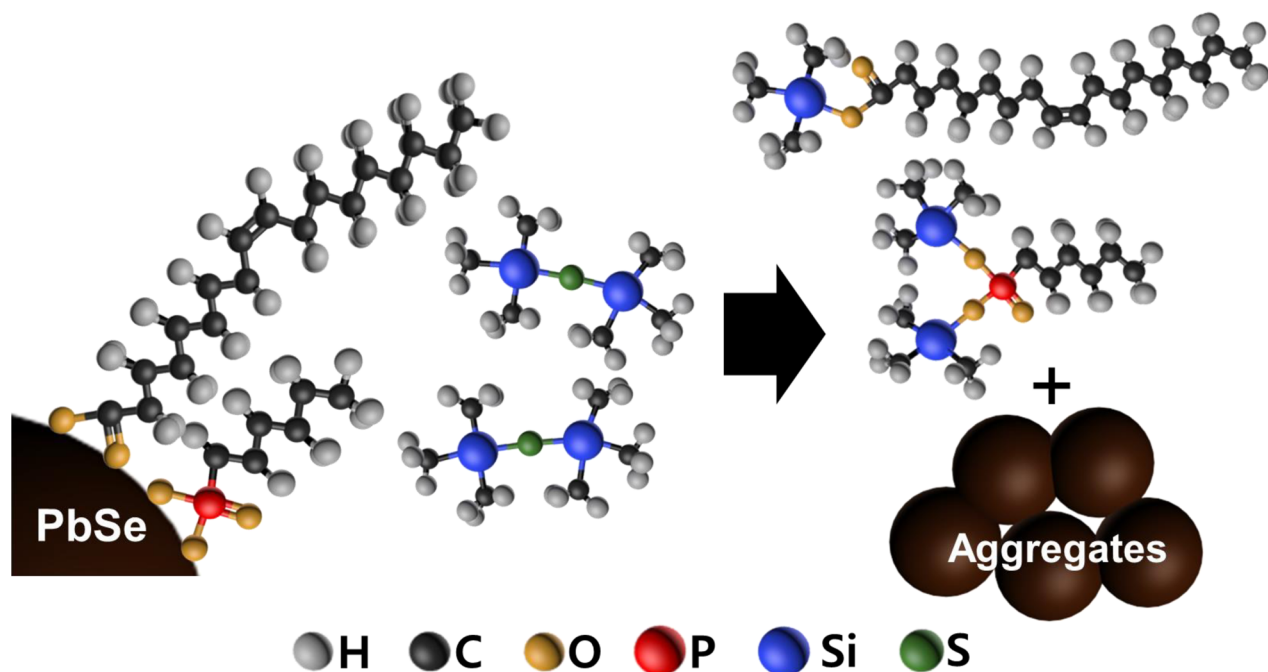


Figure 3. $^{31}\text{P}\{^1\text{H}\}$ NMR spectra of fresh (A) TDP-PbSe NCs and (B) TOP-PbSe NCs dispersed in benzene-*d*₆. (C) $^{31}\text{P}\{^1\text{H}\}$ NMR spectrum of TDP-PbSe NCs after ligand cleavage reaction by addition of (TMS)₂S. The sharp peaks can be assigned to silanized species of TDP derivatives.

ligand cleavage reaction occurs via silanization.^{28,29} Considering those studies, ligand cleavage results in our TDP-PbSe NCs are expected to derive from silanization (Scheme 1). Then, phosphorus-containing TDP derivatives on TDP-PbSe NC surfaces likely have P–O– moieties, which account for the enhanced air stability of TDP-PbSe NCs. Indeed, the existence of P–O– moieties in TDP-PbSe NCs is confirmed by FTIR spectra shown in Figure S7. The number of oleates per NC was largely unaltered between the cases of TOP- and TDP-PbSe NCs, indicating the TDP derivatives passivate the surface atoms that are not bound to oleate (Figure S5).

The NMR and FTIR analyses strongly indicate that during the synthesis of TDP-PbSe NCs, TDP transforms into its derivatives forming P–O– moieties which passivate the surface of PbSe NC. Hydrolysis of TDP²⁵ during the synthesis of TDP-PbSe NCs may have to do with formation of molecules carrying P–O– moieties. As P–O– moieties are confirmed to form in our TDPSe-based synthesis, we turn our attention to previous synthetic procedures that involved TDPSe for the growth of PbSe nanomaterials. The interaction of P–O– moieties with surface of PbSe may play a significant role in the growth of PbSe NRs using TDP.^{24,25} In addition, the synthesis of PbSe

Scheme 1. Schematic Illustration of Ligand Cleavage Reaction in PbSe NCs Passivated by P–O– Moiety after Reacting with $(\text{TMS})_2\text{S}^a$



^aOriginally, the surface of PbSe NC is passivated by ligands with P–O– moiety and oleate ligands together. Upon adding $(\text{TMS})_2\text{S}$ to NC solution, oleate and P–O– moiety are cleft out by silanization and NCs form aggregations. HPA is taken as an example of ligand with P–O– moiety.

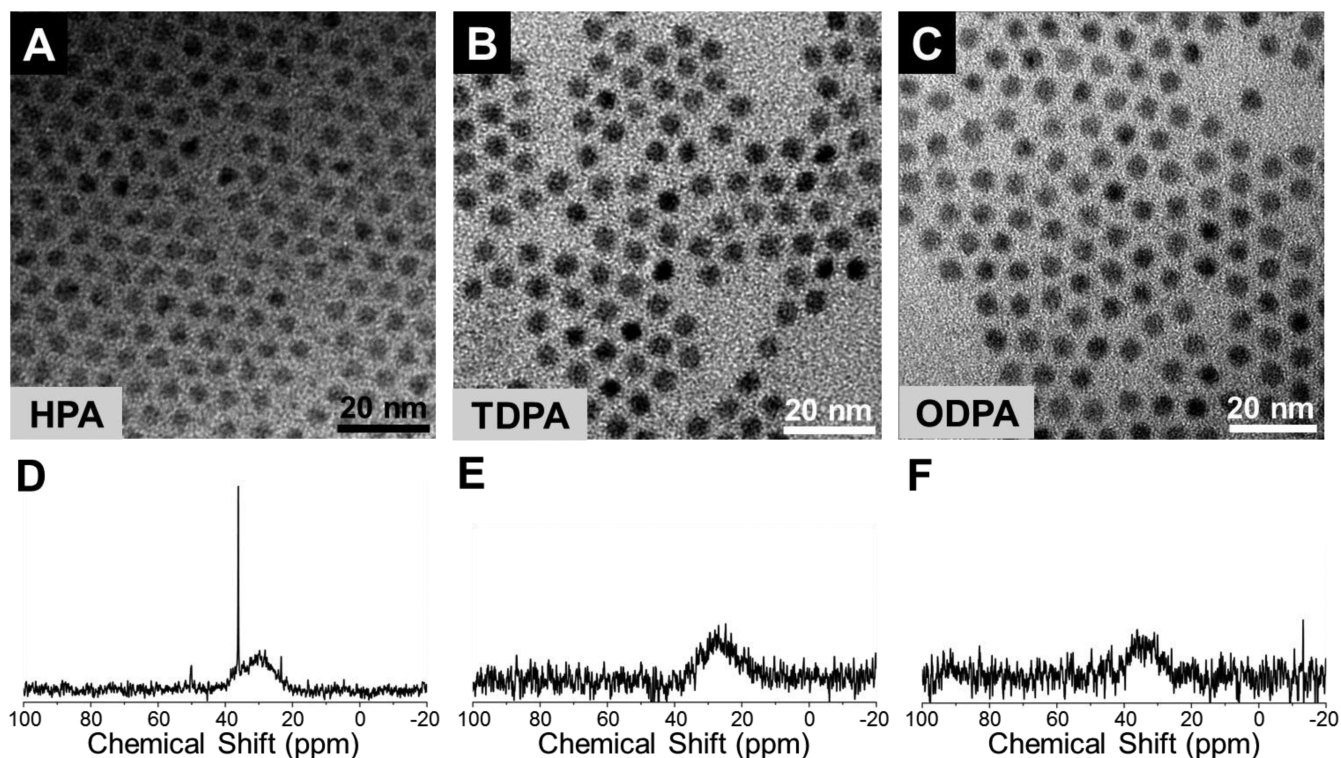


Figure 4. TEM images of (A) HPA-, (B) TDPA-, and (C) ODPA-PbSe NCs. $^{31}\text{P}\{^1\text{H}\}$ NMR spectra of (D) HPA-, (E) TDPA-, and (C) ODPA-PbSe NCs. Sharp resonance at 36.2 ppm in (D) is the peak of residual free HPA.

nanowires (NWs) using PAs as the ligands highlights the correlation between ligand–surface interaction and morphology of the resulting PbSe nanomaterials.^{32,33}

As we surmise that passivation by P–O– moieties has to do with the enhanced air stability of PbSe NCs, we synthesized

PbSe NCs using PAs (denoted as PA-PbSe NCs) and examined the stability of the resulting NCs. Hexylphosphonic acid (HPA), tetradecylphosphonic acid (TDPA), or octadecylphosphonic acid (ODPA) was introduced at the step of Pb-oleate preparation or TOPSe injection (see [Experimental](#)

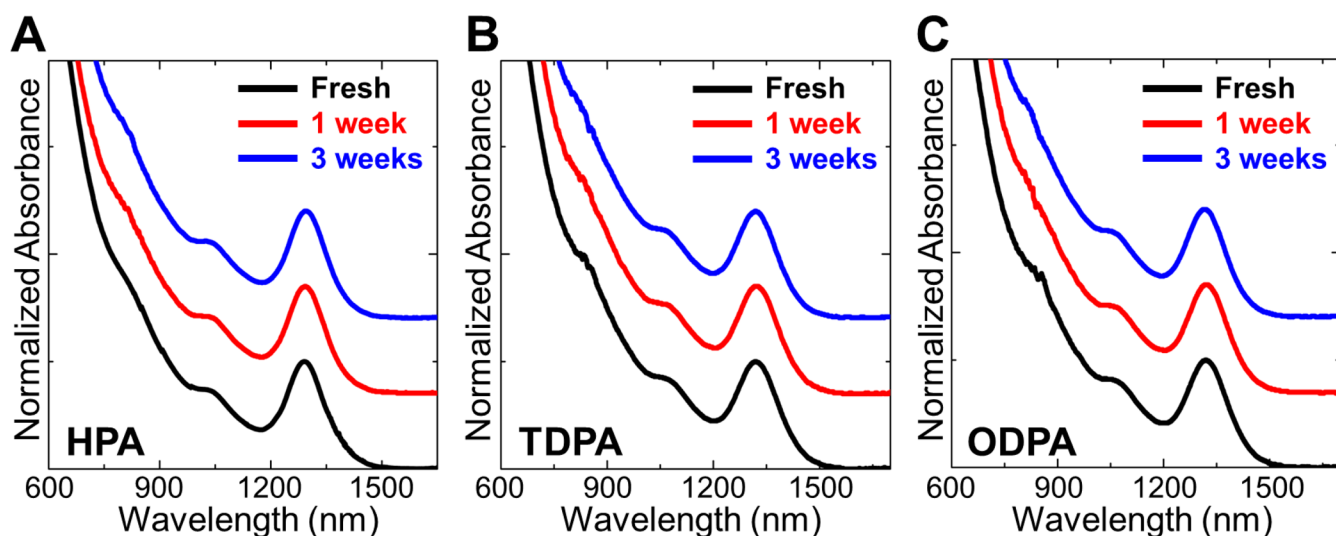


Figure 5. Absorption spectra of (A) HPA-, (B) TDPA-, and (C) ODPA-PbSe NCs dispersed in tetrachloroethylene. Absorption spectra were recorded for 3 weeks with air exposure in ambient condition.

Section for details). In our synthetic procedures, the resulting PA-PbSe NCs were in spherical shape in all three cases of PAs as shown in Figure 4A–C. $^{31}\text{P}\{^1\text{H}\}$ NMR spectroscopy reveals that singlet, surface bound broad resonance ranged in 10–40 ppm of chemical shift for all PA-PbSe NCs (Figure 4D–F).

To investigate ambient stability of PA-PbSe NCs, we stored the NCs under ambient condition (see Experimental Section for details), and their absorption spectra were recorded over time. The shapes and peak positions of absorption spectra for all our PA-PbSe NCs remained nearly intact for more than 3 weeks of air exposure (Figure 5A–C). The long-term air stability of PA-PbSe NCs corroborates our hypothesis that the surface bound P–O– moieties account for the enhanced stability. The interactions of PAs with surface atoms have been intensively studied in the case of CdSe NCs.^{28,29} However, surface chemistry of the PA-PbSe NC has not been reported to date, although there have been a few reports describing approaches to synthesizing Pb chalcogenide nanomaterials of varying morphologies using PAs.^{32–34} To the best of our knowledge, this is the first report that PAs help enhance air stability of PbSe NCs.

From the X-ray photoelectron spectroscopy (XPS) analysis, it was revealed that P–O– moieties passivate the Pb. On the other hand, we have found nearly no evidence of Se passivation by P–O– moieties (Figure S8). Still, TDP- and PA-PbSe NCs underwent much less Se oxidation compared to their counterpart, TOP-PbSe NCs (Figure S9). Suppressed Se oxidation might have originated from the effective passivation of Pb dangling bonds, where oxidation can be initiated and propagated, by P–O– moieties.

In order to examine the stability of PbSe NCs in a device form, we prepared field effect transistors (FETs) based on PbSe NCs synthesized using different capping ligands. Figure 6 shows the transfer curves of FETs fabricated using TOP- and HPA-PbSe NCs (see Figure S10 for transfer curves swept in both directions). FETs were fabricated with NC solutions with and without air exposure, and then transfer curves were recorded (see Experimental Section for a detailed method of FET stability test). For a TOP-PbSe NC FET, the transfer curve shifted to more positive gate voltage (V_G) value after air exposure, indicating hole doping by oxygen (Figure 6A).³⁸ In

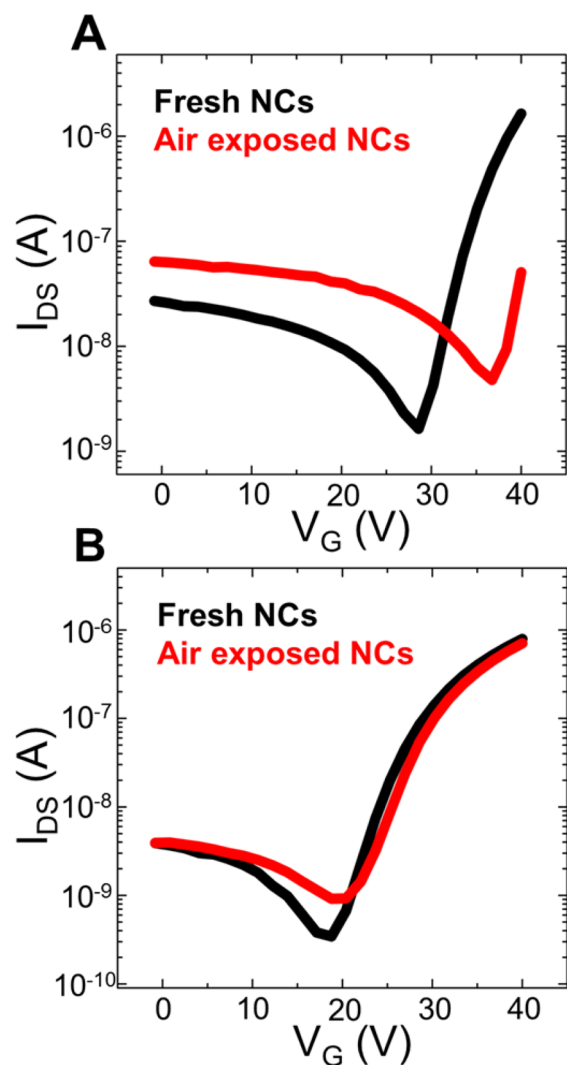


Figure 6. Transfer curves of (A) TOP- and (B) HPA-PbSe NC field effect transistors (FETs). Black and red lines indicate transfer curves of fresh and 4 days air exposed NCs, respectively. 10 V of drain-source voltage was applied.

contrast, transfer curves of HPA-PbSe NC FET are nearly intact preserving their initial characteristics even after the exposure of nanocrystals solution to air for 4 days (Figure 6B). It is worthy to note that the operation of the FET based on HPA-PbSe NCs exhibited distinct ambipolar characteristics, similar to the case of TOP-PbSe NCs, whereas halide-treated PbSe NCs shows strong n-type characteristics (Figure S11).¹⁰ As such, the PA-PbSe NCs and TDP-PbSe NCs represent a new class of materials because they exhibit air stability without significant change in doping polarity from TOP-PbSe NCs.

CONCLUSION

In conclusion, we have developed a new simple strategy to dramatically improve the stability of PbSe NCs: replacing Se precursor for the synthesis. TDPSe was introduced to Pb oleate solution as a Se source, and the resulting PbSe NCs (TDP-PbSe NCs) showed markedly enhanced stability. ³¹P{¹H} and ¹H NMR analyses reveal that surface of TDP-PbSe NCs are passivated by TDP derivatives as well as oleates. From the ligand cleavage reaction using (TMS)₂S, it was observed that TDP derivatives are bound with P–O– moieties on the surface of PbSe NCs, which was also confirmed by FTIR analysis. To verify the role of P–O– moieties, we used PAs as additional capping ligands in the synthesis of PbSe NCs, which resulted in air-stable PbSe NCs (PA-PbSe NCs). In contrast to the halide-based surface treatment approach exercised in recent reports, this new agenda enables the preparation of air-stable PbSe NCs with inherent ambipolar FET characteristics.

We note that stability improvement strategy using PAs has promising potential to be applied in air-stable NC-based electronic applications. To fabricate NC-based solar cells, bulky surface ligands are typically replaced with short molecular linkers such as 1,2-ethanedithiol (EDT) or 3-mercaptopropionic acid (MPA). Such ligand exchange with small molecular linkers enhances the interparticle coupling and results in the facilitated charge transfer between NCs. Small, bifunctional molecules with P–O– moieties may serve as molecular linkers in the place of EDT or MPA in NC film fabrications, potentially addressing the prevalent issues of stability, or lack thereof, of NC films in NC-based solid state devices.

EXPERIMENTAL SECTION

General Considerations. For material synthesis, standard Schlenk-line techniques were used unless described otherwise. Lead(II) oxide (PbO, 99.999%, Aldrich), selenium shot (Se, 99.999+, Alfa Aesar), 1-octadecene (ODE, technical grade, Aldrich), oleic acid (OA, technical grade and 99% from Aldrich and Alfa Aesar, respectively), trioctylphosphine (TOP, 90%, Aldrich, Lot # WXBB4938 V), tris(diethylamino)phosphine (TDP, 98%, Alfa Aesar), *n*-hexylphosphonic acid (HPA, Alfa Aesar), 1-tetradecylphosphonic acid (TDPA, 98%, Alfa Aesar), *n*-octadecylphosphonic acid (ODPA, 97%, Alfa Aesar), and tetrachloroethylene (TCE, ≥99%, Aldrich) were purchased and used without further purifications.

Characterization. For absorption spectroscopy measurement, samples were dispersed in TCE and spectra were recorded using a Shimadzu UV–vis–NIR 3600 spectrophotometer. Optical density of the 1S exciton peak was set below 0.2 to minimize optical interaction among NCs. For transmission electron microscopy (TEM) analysis, PbSe NC solution in hexane was drop-cast on a 200-mesh carbon-coated copper grid, and images were obtained using a Tecnai F20 (200 kV) and a Tecnai TF30 ST (300 kV) electron microscope. For NMR analysis, all NC samples were dispersed in benzene-*d*₆. NC solution of 0.8–1.0 mL was taken and transferred to a NMR tube for measurement, and then the tube was tightly sealed using Parafilm. All these procedures were conducted in a N₂-filled glovebox. Shortly

prior to measurement, we took the samples out of the glovebox, and NMR spectra were recorded by an Agilent 400 MHz 54 mm NMR DD2. H₃PO₄ was used as an external reference for ³¹P{¹H} NMR measurement, and solvent (benzene-*d*₆) was used as a reference for ¹H NMR measurement. For XRD analysis, PbSe NC hexane solution was drop-cast on a glass substrate and was let dried. We repeated these steps for several times until a thick PbSe NC film is obtained. XRD spectra were recorded using a Rigaku Ultima IV. FTIR spectra were recorded using an Alpha FTIR spectrometer (Bruker). IV curves for FETs were collected using a B2902A precision source/measure unit (Agilent) in a N₂-filled glovebox. XPS data were obtained using PHI Quantera-II spectrometer with aluminum anode (Al Kα = 1486.7 eV). PL spectra were obtained using PL spectrometer (Fluorolog, Horiba Jobin Yvon Inc.).

Synthesis of TOP-PbSe NCs. TOP-PbSe NCs were synthesized following a previously reported method with slight modifications.²² Typically, 0.22 g of PbO (1.0 mmol), 2.8 mL of OA (technical grade, Aldrich, 8.0 mmol), and 2.5 mL of ODE or diphenyl ether were mixed in a round-bottom three-neck flask, which was placed on a heating mantle. Then temperature was raised to 100 °C and degassed under vacuum for 2–3 h. During degassing, the solution turned transparent, which is indicative of Pb-oleate formation. After that, the temperature was set to reaction temperature (120–180 °C), and 3 mL of 2 M TOPSe was rapidly injected. Finally, the mixture was quenched in a water bath after desired reaction time (5–20 min). Crude reaction solution was centrifuged at 6000 rpm for 5 min with addition of acetone and methanol and then redispersed in hexane. Again, this solution was centrifuged at 6000 rpm for 5 min after adding acetone and methanol and then redispersed in hexane, TCE, or benzene-*d*₆ for further characterizations.

Synthesis of TDP-PbSe NCs. TDP-PbSe NCs were synthesized based on a previous method reported with some modifications.^{22,24} Typically, 0.22 g of PbO (1.0 mmol), 0.65 mL of OA (99%, Alfa Aesar, 2.0 mmol), and 5 mL of ODE were loaded in a round-bottom three-neck flask. The flask was degassed at 100 °C for 2–3 h (initially, degassing time was varied from 2 to 24 h, but nearly no difference was observed) and then heated to reaction temperature (140–190 °C). When temperature is stabilized, 0.31 mL of 3 M TDPSe was swiftly injected and maintained for certain period of reaction time (2–20 min). At the end of the reaction, the flask was cooled to room temperature using a water bath. TDP-PbSe NCs were collected with centrifugation of 2 times by adding acetone and methanol. After that, TDP-PbSe NCs were dispersed in hexane, TCE, or benzene-*d*₆ for further characterizations.

Synthesis of PbSe NRs. PbSe NRs were synthesized using previously reported method with some modifications.^{24,25} 0.47 g of PbO (2.1 mmol), 1.5 mL of OA (99%, Alfa Aesar, 4.7 mmol), and 10 mL of ODE were loaded in a round-bottom three-neck flask. The flask was degassed for 2–3 h at 100 °C, and then temperature was increased to 120 °C under nitrogen flow. After that, 2.1 mL of 3 M TDPSe was rapidly injected. The reaction time was adjusted (2–5 min) depending on desired size. Finally, the flask was cooled by removing the heating mantle, and the reaction solution was centrifuged for 2 times by adding the mixture of acetone and methanol.

Synthesis of PA-PbSe NCs. For HPA-PbSe NCs, 0.22 g of PbO (1.0 mmol), 2.8 mL of OA (technical grade, Aldrich, 8.0 mmol), and 2.5 mL of ODE were loaded in a round-bottom three-neck flask (1). Also, 0.05 g of HPA (0.3 mmol) in 2.5 mL of ODE was prepared in another round-bottom three-neck flask (2). Both flasks were degassed for 2–3 h at 100 °C, and then temperatures of (1) and (2) were increased to 140 and 150 °C under nitrogen flow, respectively. 3 mL of 2 M TOPSe was swiftly injected to (1), which is directly followed by rapid injection of 2.5 mL of HPA ODE solution. (1) was kept at 140 °C for the desired reaction time and then cooled in a water bath. With the reaction time of 20 min, HPA-PbSe NCs with 1S exciton peak position around 1300 nm was obtained. For the synthesis of TDPA-PbSe NCs, 0.22 g of PbO (1.0 mmol), 2.8 mL of OA (technical grade, Aldrich, 8.0 mmol), 0.08 g of TDPA (0.3 mmol), and 2.5 mL of ODE were loaded in a round-bottom three-neck flask. After degassing of 2–3 h at 100 °C, temperature was increased to 150 °C. Then 3 mL of 2

M TOPSe was rapidly injected. After the reaction for 10 min, flask was quenched in water bath. Finally, TDPA-PbSe NCs with 1S exciton peak position around 1300 nm was obtained. For the synthesis of ODPA-PbSe NCs, all precursors were loaded in same manner with the synthesis of TDPA-PbSe NCs except PA. Instead of 0.08 g of TDPA (0.3 mmol), equimolar ODPA (0.10 g, 0.3 mmol) was loaded, and all reaction parameters were also kept identically with the synthesis of TDPA-PbSe NCs. All PA-PbSe NCs were centrifuged for 2 times at 6000 rpm with addition of acetone.

Solution Stability Test. PbSe NCs were dispersed in TCE and stored in vials with loose capping, and the vials were left under ambient condition with room light. Right before collecting absorption spectra, PbSe NCs solution was diluted again in TCE, and then characterization was carried out.

Oleate Ligand Coverage Calculation. PbSe NCs were dispersed in benzene- d_6 , and ferrocene (2 mM) was used as an internal reference. Concentrations of NC were derived from absorption spectra and absorption coefficient using the Beer–Lambert law.^{35,36} Oleate ligand density was calculated by comparing the integrated area of oleate (vinylic hydrogen) and ferrocene in ¹H NMR spectra. The peaks of bound oleate were extracted by Lorentzian fitting.¹⁰

FET Fabrication. PbSe NCs were dispersed in anhydrous octane (10 mg/mL). PbSe NC films were deposited on Si substrates (interdigitated Cr/Au electrode, thickness of SiO₂ was 500 nm) via layer-by-layer spin coating as reported in a previous study with slight modifications.³⁷ 2–3 drops of NC octane solution were dropped on a substrate which is followed by ligand exchange with MPA solution (1 vol % in acetonitrile). Then acetonitrile, methanol, and octane were sequentially dropped on the film for rinsing. This cycle was repeated for 5 times, and all spin-coating procedures were performed at 2500 rpm and in a N₂-filled glovebox.

FET Stability Test. First, FET was fabricated with fresh NCs, and then IV curves were recorded. After that, NC solutions were stored under ambient atmosphere in loosely capped vials. After some period of time, FET was fabricated again with air-exposed NCs, and then IV curves were recorded.

PL QY Estimation. PL QY of PbSe NCs was estimated by comparing to IR-26. PL QY of IR-26 was assumed 0.03% when the optical density was set around 1.³⁹

■ ASSOCIATED CONTENT

Supporting Information

The Supporting Information is available free of charge on the ACS Publications website at DOI: 10.1021/jacs.5b10273.

TEM, absorption spectra, NMR, FTIR, XPS, PL, and FET data (PDF)

■ AUTHOR INFORMATION

Corresponding Authors

*E-mail sjeong@kimm.re.kr (S.J.).

*E-mail dcllee@kaist.edu (D.C.L.).

Notes

The authors declare no competing financial interest.

■ ACKNOWLEDGMENTS

This work was supported by the Global R&D program (1415134409) funded by KIAT and the Global Frontier R&D program by the Center for Multiscale Energy Systems (2011-0031566). D.C.L. was supported by grants 2011-0030256 and 2014RIA2A2A01006739, and J.Y.W. was also supported by grant 2015H1A2A1034211 from National Research Foundation (NRF) funded by the Korean government.

■ REFERENCES

(1) Wise, F. W. *Acc. Chem. Res.* **2000**, *33*, 773.

(2) Du, H.; Chen, C. L.; Krishnan, R.; Krauss, T. D.; Harbold, J. M.; Wise, F. W.; Thomas, M. G.; Silcox, J. *Nano Lett.* **2002**, *2*, 1321.

(3) Ellingson, R. J.; Beard, M. C.; Johnson, J. C.; Yu, P. R.; Mícić, O. I.; Nozik, A. J.; Shabaev, A.; Efros, A. L. *Nano Lett.* **2005**, *5*, 865.

(4) Semonin, O. E.; Luther, J. M.; Choi, S.; Chen, H. Y.; Gao, J. B.; Nozik, A. J.; Beard, M. C. *Science* **2011**, *334*, 1530.

(5) Nozik, A. J.; Beard, M. C.; Luther, J. M.; Law, M.; Ellingson, R. J.; Johnson, J. C. *Chem. Rev.* **2010**, *110*, 6873.

(6) Schaller, R. D.; Klimov, V. I. *Phys. Rev. Lett.* **2004**, *92*, 186601.

(7) Choi, J. J.; Lim, Y. F.; Santiago-Berrios, M. B.; Oh, M.; Hyun, B. R.; Sung, L. F.; Bartnik, A. C.; Goedhart, A.; Malliaras, G. G.; Abruna, H. D.; Wise, F. W.; Hanrath, T. *Nano Lett.* **2009**, *9*, 3749.

(8) Qi, D.; Fischbein, M.; Drndić, M.; Šelmić, S. *Appl. Phys. Lett.* **2005**, *86*, 093103.

(9) Luther, J. M.; Beard, M. C.; Song, Q.; Law, M.; Ellingson, R. J.; Nozik, A. J. *Nano Lett.* **2007**, *7*, 1779.

(10) Woo, J. Y.; Ko, J. H.; Song, J. H.; Kim, K.; Choi, H.; Kim, Y. H.; Lee, D. C.; Jeong, S. *J. Am. Chem. Soc.* **2014**, *136*, 8883.

(11) Bae, W. K.; Joo, J.; Padilha, L. A.; Won, J.; Lee, D. C.; Lin, Q. L.; Koh, W. K.; Luo, H. M.; Klimov, V. I.; Pietryga, J. M. *J. Am. Chem. Soc.* **2012**, *134*, 20160.

(12) Sykora, M.; Kopusov, A. Y.; McGuire, J. A.; Schulze, R. K.; Tretiak, O.; Pietryga, J. M.; Klimov, V. I. *ACS Nano* **2010**, *4*, 2021.

(13) Leschkes, K. S.; Kang, M. S.; Aydil, E. S.; Norris, D. J. *J. Phys. Chem. C* **2010**, *114*, 9988.

(14) Oh, S. J.; Berry, N. E.; Choi, J. H.; Gauldin, E. A.; Lin, H. F.; Paik, T.; Diroll, B. T.; Muramoto, S.; Murray, C. B.; Kagan, C. R. *Nano Lett.* **2014**, *14*, 1559.

(15) Pietryga, J. M.; Werder, D. J.; Williams, D. J.; Casson, J. L.; Schaller, R. D.; Klimov, V. I.; Hollingsworth, J. A. *J. Am. Chem. Soc.* **2008**, *130*, 4879.

(16) Zhang, J. B.; Gao, J. B.; Miller, E. M.; Luther, J. M.; Beard, M. C. *ACS Nano* **2014**, *8*, 614.

(17) Zhang, J. B.; Gao, J. B.; Church, C. P.; Miller, E. M.; Luther, J. M.; Klimov, V. I.; Beard, M. C. *Nano Lett.* **2014**, *14*, 6010.

(18) Kim, S.; Marshall, A. R.; Kroupa, D. M.; Miller, E. M.; Luther, J. M.; Jeong, S.; Beard, M. C. *ACS Nano* **2015**, *9*, 8157.

(19) Ning, Z. J.; Voznyy, O.; Pan, J.; Hoogland, S.; Adinolfi, V.; Xu, J. X.; Li, M.; Kirmani, A. R.; Sun, J. P.; Minor, J.; Kemp, K. W.; Dong, H. P.; Rollny, L.; Labelle, A.; Carey, G.; Sutherland, B.; Hill, I. G.; Amassian, A.; Liu, H.; Tang, J.; Bakr, O. M.; Sargent, E. H. *Nat. Mater.* **2014**, *13*, 822.

(20) Ning, Z. J.; Ren, Y.; Hoogland, S.; Voznyy, O.; Levina, L.; Stadler, P.; Lan, X. Z.; Zhitomirsky, D.; Sargent, E. H. *Adv. Mater.* **2012**, *24*, 6295.

(21) Ning, Z. J.; Dong, H. P.; Zhang, Q.; Voznyy, O.; Sargent, E. H. *ACS Nano* **2014**, *8*, 10321.

(22) Murray, C. B.; Sun, S. H.; Gaschler, W.; Doyle, H.; Betley, T. A.; Kagan, C. R. *IBM J. Res. Dev.* **2001**, *45*, 47.

(23) Koh, W. K.; Yoon, Y.; Murray, C. B. *Chem. Mater.* **2011**, *23*, 1825.

(24) Koh, W. K.; Bartnik, A. C.; Wise, F. W.; Murray, C. B. *J. Am. Chem. Soc.* **2010**, *132*, 3909.

(25) Boercker, J. E.; Foos, E. E.; Placencia, D.; Tischler, J. G. *J. Am. Chem. Soc.* **2013**, *135*, 15071.

(26) Choi, H.; Ko, J. H.; Kim, Y. H.; Jeong, S. *J. Am. Chem. Soc.* **2013**, *135*, 5278.

(27) Bealing, C. R.; Baumgardner, W. J.; Choi, J. J.; Hanrath, T.; Hennig, R. G. *ACS Nano* **2012**, *6*, 2118.

(28) Owen, J. S.; Park, J.; Trudeau, P. E.; Alivisatos, A. P. *J. Am. Chem. Soc.* **2008**, *130*, 12279.

(29) Gomes, R.; Hassinen, A.; Szczygiel, A.; Zhao, Q. A.; Vantomme, A.; Martins, J. C.; Hens, Z. *J. Phys. Chem. Lett.* **2011**, *2*, 145.

(30) Joung, S.; Yoon, S.; Han, C. S.; Kim, Y.; Jeong, S. *Nanoscale Res. Lett.* **2012**, *7*, 93.

(31) Dean, J. A. *Lange's Handbook of Chemistry*, 15th ed.; McGraw-Hill: New York, 1999.

(32) Cho, K. S.; Talapin, D. V.; Gaschler, W.; Murray, C. B. *J. Am. Chem. Soc.* **2005**, *127*, 7140.

- (33) Foos, E. E.; Zega, T. J.; Tischler, J. G.; Stroud, R. M.; Boercker, J. E. *J. Mater. Chem.* **2011**, *21*, 2616.
- (34) Mokari, T. L.; Zhang, M. J.; Yang, P. *J. Am. Chem. Soc.* **2007**, *129*, 9864.
- (35) Dai, Q.; Wang, Y.; Li, X.; Zhang, Y.; Pellegrino, D. J.; Zhao, M.; Zou, B.; Seo, J. T.; Wang, Y.; Yu, W. W. *ACS Nano* **2009**, *3*, 1518.
- (36) Moreels, I.; Lambert, K.; De Muynck, D.; Vanhaecke, F.; Poelman, D.; Martins, J. C.; Allan, G.; Hens, Z. *Chem. Mater.* **2007**, *19*, 6101.
- (37) Ip, A. H.; Thon, S. M.; Hoogland, S.; Voznyy, O.; Zhitomirsky, D.; Debnath, R.; Levina, L.; Rollny, L. R.; Carey, G. H.; Fischer, A.; Kemp, K. W.; Kramer, I. J.; Ning, Z. J.; Labelle, A. J.; Chou, K. W.; Amassian, A.; Sargent, E. H. *Nat. Nanotechnol.* **2012**, *7*, 577.
- (38) Leschkies, K. S.; Kang, M. S.; Aydil, E. S.; Norris, D. J. *J. Phys. Chem. C* **2010**, *114*, 9988.
- (39) Semonin, O. E.; Johnson, J. C.; Luther, J. M.; Midgett, A. G.; Nozik, A. J.; Beard, M. C. *J. Phys. Chem. Lett.* **2010**, *1*, 2445.